Unconventional spin fluctuations in the hexagonal antiferromagnet $YMnO_3$

T. J. Sato,[1,*] S. -H. Lee,[1] T. Katsufuji,[2] M. Masaki,[3] S. Park,[1,4] J. R. D. Copley,[1] and H. Takagi[3]
[1]*NIST Center for Neutron Research, National Institute of Standards and Technology, Gaithersburg, Maryland 20899, USA*
[2]*Department of Physics, Waseda University, Shinjuku-ku, Tokyo 169-8555, Japan*
[3]*Department of Advanced Materials Science and Department of Applied Chemistry, University of Tokyo, Tokyo 113-8656, Japan*
[4]*Department of Materials and Nuclear Engineering, University of Maryland, College Park, Maryland 20742, USA*
(Received 18 April 2003; published 30 July 2003)

We used inelastic neutron scattering to show that well below its Néel temperature, T_N, the two-dimensional (2D) *XY* nearly triangular antiferromagnet $YMnO_3$ has a prominent *central peak* associated with 2D antiferromagnetic fluctuations with a characteristic lifetime of 0.55(5) ps, coexisting with the conventional long-lived spin waves. Existence of the two time scales suggests competition between the Néel phase favored by weak interplane interactions, and the Kosterlitz-Thouless phase intrinsic to the 2D *XY* spin system.

DOI: 10.1103/PhysRevB.68.014432 PACS number(s): 75.30.Ds, 75.25.+z, 75.40.Gb, 75.50.Ee

I. INTRODUCTION

Geometrical frustration and low dimensionality are the two key concepts in the statistical physics that provide unusual spin dynamics as well as phase transitions.[1–3] The simplest realization of the two concepts is two-dimensional triangular lattice antiferromagnets (2DTLAFMs). A particular interest is placed on the *XY* spin system (2D*XY*TLAFM), where its ground-state manifold has the continuous degeneracy associated with U(1) global spin rotations, as well as the discrete Ising-like degeneracy due to Z_2 chirality configurations.[4] Because of the U(1) symmetry, the well-known Kosterlitz-Thouless (KT) phase involving vortex binding[5] is expected at low temperatures. Experimentally, little evidence can be found in the literature due to the lack of good model systems.[6]

Rare-earth manganites $R\mathrm{MnO_3}$ (R=Y, Lu, and Sc) are ferroelectric compounds with considerably high ferroelectric Curie temperature above 1000 K.[7] Below the ferroelectric transition, these compounds crystallize in a hexagonal structure with the space group $P6_3cm$. The Mn^{3+} ($S=2$) ions are at the $6c(x,0,0)$ positions [$x=0.323(1)$ for R=Y (Ref. 7)], forming nearly triangular networks in $z=0$ and 1/2 layers. These layers stack in the ABAB sequence along the z axis (see Fig. 1),[7–9] with a wide separation introduced by intervening R and O ions. This wide separation suggests predominant two-dimensional (2D) character in the *ab* plane, and thus the $R\mathrm{MnO_3}$ compounds can be good candidates for the 2DTLAFMs. Their bulk susceptibility data show that despite strong antiferromagnetic interactions the magnetic ions order long range at much lower temperatures T_N than the magnetic energy scale inferred by the Curie-Weiss (CW) temperatures Θ_{CW} (for instance, $\Theta_{CW}=-705$ K and $T_N=70$ K for $YMnO_3$).[7–9] Previous powder neutron-diffraction studies showed that the spins at the lowest temperature formed the so-called 120° structure in the *ab* plane coinciding with the ground state for 2DTLAFMs, and the frozen moments, $\langle M\rangle$, were reduced from the expected value for the fully polarized Mn^{3+} [e.g., $\langle M\rangle=2.90(2)\mu_B<gS\mu_B$ for $YMnO_3$ ($S=2$)].[7,8,10] The reduction in T_N and $\langle M\rangle$ is a signature of strong spin fluctuations due to geometrical frustration and/or low dimensionality in the systems. The low T_N, compared to the ferroelectric transition temperature, also infers weak coupling between the magnetism and ferroelectricity. In the powder neutron-diffraction pattern, a broad peak was additionally observed at finite Q around T_N, indicative of strong short-range spin correlations.[7,10] However, due to intrinsic limitations of the powder-diffraction technique, further experimental studies, especially inelastic single-crystal neutron-scattering measurements, are necessary to understand the nature of the spin excitations.

In this paper, we report inelastic neutron-scattering measurements on powder and single-crystal samples of the hexagonal rare-earth manganite $YMnO_3$. We have found that $YMnO_3$ is a good model system for the 2D*XY*TLAFM with weak trimerization. Our most important finding is that in the Néel phase there are fast 2D spin fluctuations with a characteristic time scale of 0.55(5) ps in addition to the conventional long-lived spin-wave (SW) excitations. The inverse of dynamic correlation length associated with the fast 2D spin fluctuations has similar T dependence as that expected for the KT phase in a 2D *XY* spin system, suggesting that the spin fluctuations are reminiscence of the KT phase. The coexistence of the long-lived magnons and the fast 2D spin fluctua-

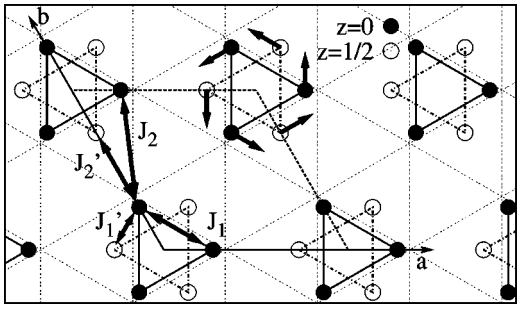

FIG. 1. Schematic drawing of Mn positions and spin ordering in $YMnO_3$. Filled (open) circles represent Mn positions in the $z=0$ ($z=1/2$) plane, whereas the dotted parallelogram shows the magnetic unit cell that is identical to the chemical unit cell. Lattice constants are $a=6.140$ Å and $c=11.393$ Å. The lattice is weakly trimerized with the intratrimer and intertrimer Mn-Mn distances of 3.42 Å and 3.62 Å, respectively (Refs. 7 and 9) which is exaggerated in the drawing.

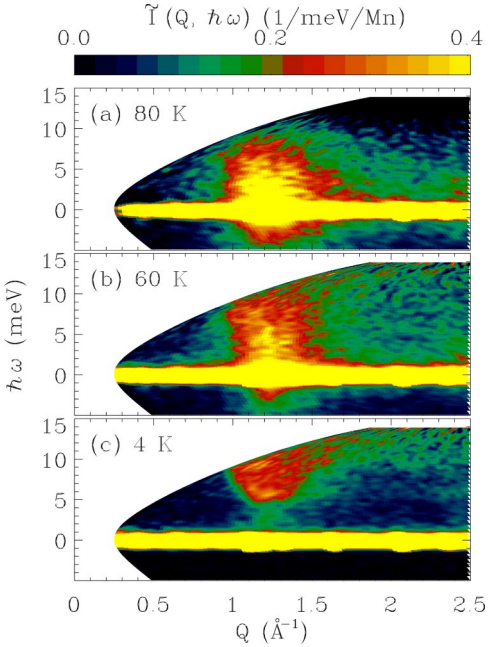

FIG. 2. (Color online) Contour maps of the powder-averaged neutron-scattering intensity versus magnitude of wave-vector transfer Q and energy transfer $\hbar\omega$ at three different temperatures spanning the phase transition at $T_N=70$ K.

tions also suggests competition between the Néel phase and the KT phase in this quasi-2D *XY* spin system.

II. EXPERIMENT

A 50-g powder sample and a 2-g (ϕ5 mm×22 mm) single crystal of $YMnO_3$ were used in our neutron-scattering measurements. Methods of sample preparation were reported elsewhere.[9] Neutron-scattering measurements were performed at the National Institute of Standards and Technology (NIST) Center for Neutron Research. Powder experiments were performed at the Disk Chopper time-of-flight Spectrometer (DCS) using an incident energy of $E_i=15.46$ meV and single-crystal experiments at the cold neutron triple-axis spectrometer (SPINS) and the thermal-neutron triple-axis spectrometer BT9. At SPINS, pyrolytic graphite (PG) 002 reflections were used for monochromator and analyzer, and a cooled Be filter was placed after the sample to eliminate higher-order contamination. We used horizontal collimations of $80'-80'$ and a final energy $E_f=5$ meV for most scans, while $E_f=2.6$ meV and $80'-40'$ were used when better energy resolution was needed. At BT9, the PG monochromator and analyzer were used with $E_f=14.7$ meV, and a PG filter was used to get rid of higher-order contamination. The horizontal collimations were $40'-40'-40'-80'$.

III. RESULTS AND DISCUSSION

Figure 2 provides an overview of the inelastic neutron-scattering intensity $\tilde{I}(Q,\omega)$ for the powder sample at three temperatures. The powder-averaged scattering intensity is related to the dynamic spin-correlation function $\mathcal{S}^{\alpha\beta}(\vec{Q},\omega)$ as[11]

$$\tilde{I}(Q,\omega)=\int \frac{d\Omega_{\hat{Q}}}{4\pi}\left|\frac{g}{2}F(Q)\right|^2\sum_{\alpha\beta}(\delta_{\alpha\beta}-\hat{Q}_\alpha\hat{Q}_\beta)\mathcal{S}^{\alpha\beta}(\vec{Q},\omega), \tag{1}$$

where $F(Q)$ is the magnetic form factor for Mn^{3+}. For $T>T_N$, there is a cooperative paramagnetic continuum centered at $Q=1.2$ Å^{-1} due to fluctuations of small AFM clusters, as is commonly found in geometrically frustrated AFMs.[12] By integrating $\tilde{I}(Q,\omega)$ over $\hbar\omega$ and Q, we obtained the sum rule of $S(S+1)=5.2(5)$ at 80 K, which is close to the expected value for dynamic $Mn^{3+}(S=2)$ ions. This and the Q dependence[13] tell us that the scattering is magnetic. For $T<T_N$, as the magnetic long-range order develops, spectral weight at low energies gradually shifts to higher energies. At $T=4$ K there is strong scattering above $\hbar\omega\sim5$ meV and weak scattering below.

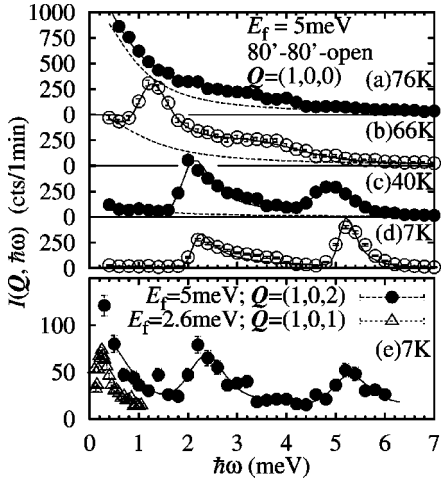

FIG. 3. (a)–(d) Constant $\vec{Q}=(1,0,0)$ scans at four different temperatures. (e) Constant-$\vec{Q}$ scans at $\vec{Q}=(1,0,2)$ and $\vec{Q}=(1,0,1)$ at $T=7$ K. The scan at $\vec{Q}=(1,0,1)$ was taken under the higher-energy-resolution configuration with $E_f=2.6$ meV, and its unit is arbitrary. Solid lines are fits to Eq. (2), whereas dashed lines represent the quasielastic part (see the text).

Next, to obtain $\vec{Q}$-directional dependence of the magnetic excitations, we have performed single-crystal inelastic-scattering experiments. Figure 3 shows the representative constant-$\vec{Q}$ scans at the antiferromagnetic zone center Γ, namely, $\vec{Q}=(1,0,0)$ and equivalent positions. For $T>T_N$, the cooperative paramagnetic continuum appears as a quasi-elastic peak centered at $\hbar\omega=0$ meV. For $T<T_N$, the quasi-elastic peak intensity decreases and two prominent magnon peaks develop at nonzero energies. The energy values of the magnon peaks increase as T decreases, becoming $\hbar\omega=2.3$ and 5.3 meV at 7 K. A constant $\vec{Q}=(1,0,1)$ scan with a better energy resolution revealed an additional mode at $\hbar\omega=0.22$ meV [Fig. 3(e)].

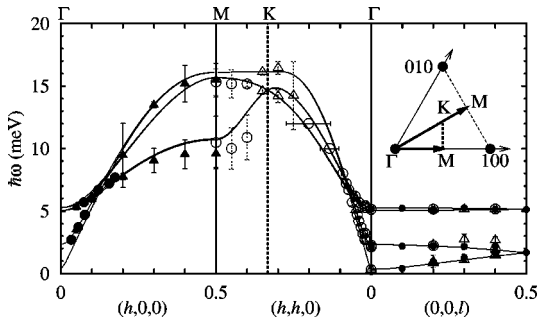

FIG. 4. Spin-wave dispersion relations along $(h,0,0)$, $(h,h,0)$, and $(0,0,l)$. Circles and triangles represent the experimentally determined peak positions. (Different marks distinguish branches appearing from different magnetic Bragg positions.) Solid lines are the model dispersion relations explained in the text. Inset: schematic drawing of scan directions in the 2D plane.

We analyzed the observed spectra using the following scattering function with Lorentzians for the quasielastic (qel) and magnon peaks:

$$\tilde{I}(\vec{Q},\hbar\omega)\propto\hbar\omega[1+n(\hbar\omega)]\left[I_{\mathrm{qel}}\frac{\Gamma_{\mathrm{qel}}}{\Gamma_{\mathrm{qel}}^2+\hbar\omega^2}+\sum_k I_{\mathrm{SW}}^k\frac{\Gamma_{\mathrm{SW}}}{\Gamma_{\mathrm{SW}}^2+(\hbar\omega-\hbar\omega_k)^2}\right], \quad (2)$$

where $[1+n(\hbar\omega)]=[1-\exp(-\hbar\omega/k_{\mathrm{B}}T)]^{-1}$. This function was convoluted with the instrumental resolution function to fit the observed spectra.

Let us first discuss the magnon dispersion relations at $T=7$ K$\ll T_{\mathrm{N}}$. Figure 4 shows the dispersion relations along a few high-symmetry directions, obtained from several constant-$\vec{Q}$ and constant-$\hbar\omega$ scans. To explain the observed dispersion relations, we introduce the following model spin Hamiltonian:

$$\mathcal{H}=-\sum_{\langle ij\rangle} J_{ij}\vec{S}_i\cdot\vec{S}_j-D_1\sum_i (S_i^z)^2-D_2\sum_i (\vec{S}_i\cdot\vec{n}_i)^2, \quad (3)$$

which consists of two in-plane (J_1 and J_2) and two interplane (J_1' and J_2') interactions, and the easy-plane (D_1) and in-plane easy-axis (D_2) anisotropies (see Fig. 1 for the definition of the interactions). The anisotropy D_2, parallel to the spin directions ($\vec{n}_i=\langle\vec{S}_i\rangle/|\langle\vec{S}_i\rangle|$), is necessary to reproduce the small (0.22 meV) gap at the antiferromagnetic zone center, and is presumably due to the local structural distortion around Mn^{3+}. The conditions $J_1'>0$ and $J_1'>J_2'$ are necessary for the particular interplane stacking in $YMnO_3$, given as the Γ_1 spin structure in Ref. 8, to be the ground state.

The model Hamiltonian is linearized using the Holstein-Primakoff approximation, and numerically diagonalized to obtain one-magnon dispersion relations using the standard equation-of-motion technique.[14] Analytic expressions for the gap energies at the Γ point were also derived assuming sufficiently small D_2, J_1', and J_2':

$$\hbar\omega_1\simeq 2S\sqrt{-D_2\lambda_1},$$

$$\hbar\omega_2\simeq 2S\sqrt{-D_2\lambda_1-2(J_1'-J_2')\lambda_1},$$

$$\hbar\omega_3\simeq S\sqrt{2(D_1\lambda_2-D_2\lambda_3-2D_1J_1')},$$

$$\hbar\omega_4\simeq S\sqrt{2[D_1\lambda_2-D_2\lambda_3-D_1(J_1'-4J_2')-2(J_1'-J_2')\lambda_2]}, \quad (4)$$

from low to high energies, where $\lambda_1=D_1+(3/2)J_1+3J_2$, $\lambda_2=(3/2)J_1+3J_2$, and $\lambda_3=2D_1+(3/2)J_1+3J_2$. Fitting the calculations to the data, we obtained $J_1=-3.4(2)$ meV, $J_2=-2.02(7)$ meV, $J_1'-J_2'=0.014(2)$ meV, $D_1=-0.28(1)$ meV, and $D_2=0.0007(6)$ meV. Solid lines in Fig. 4 represent the calculated dispersion relations with $J_2'=0$. The good agreement confirms the validity of the model Hamiltonian.

In the above paragraph, we could only determine the difference $J_1'-J_2'$ for interplane interactions. From the analytic expressions of Eq. (4), we see that $\hbar\omega_3$ and $\hbar\omega_4$ must be accurately determined in order to obtain J_1' and J_2' separately. However, this was impossible since they appear as one peak at $\hbar\omega=5.3$ meV in Fig. 3(d) or 3(e) due to the insufficient energy resolution at high energies. Since the splitting between $\hbar\omega_3$ and $\hbar\omega_4$ becomes sensitive to J_1' (or J_2') at $\vec{Q}=(1.05,0,0)$, we performed a constant-$\vec{Q}$ scan at this $\vec{Q}$ and found an almost resolution-limited peak at $\hbar\omega=5.4$ meV. This requires the splitting to be less than the energy resolution $\Delta E=0.5$ meV, and consequently an upper limit of 0.08 meV is obtained for J_1' and J_2'. Hence, the interplane interactions are at most 2.4% of the in-plane interaction J_1, confirming the good two dimensionality. One may note that $J_1\sim J_2$, which makes $YMnO_3$ rather closer to the ideal TLAFM than a system of weakly coupled trimers.

Our $J_1\simeq -3.4$ meV is one order-of-magnitude smaller than J deduced in a recent Raman-scattering study by Takahashi *et al.*[15] They obtained $J\sim -140$ cm^{-1} (~ -17 meV) by assigning a broad peak appearing at 1800 cm^{-1} ($\sim$220 meV) to two-magnon scattering. However, our results clearly show that the peak cannot be due to the two-magnon process because the bandwidth of the one-magnon branch is only about 16 meV. Their broad peak at 220 meV must be vibrational or electronic in origin rather than magnetic. There very recently also appeared a comment questioning the two-magnon origin of the broad Raman-scattering peak.[16]

Now let us turn to the low-energy quasielastic continuum observed below T_{N}, clearly seen in Figs. 3(b) and 3(c). For $T=7$ K$\ll T_{\mathrm{N}}$, Fig. 3(e) shows a $\hbar\omega=0.55$ meV mode at $\vec{Q}=(1,0,l)$ with $l\neq 0$ which is due to in-plane transverse spin fluctuations. The in-plane transverse fluctuations cannot, however, appear at $\vec{Q}=(1,0,0)$ because the polarization factor in Eq. (1) vanishes for the ordered spin structure in $YMnO_3$. Note that such a mode is not present in Fig. 3(d). Therefore we rule out the in-plane transverse spin fluctuations as the origin of the quasielastic continuum existing in the Néel phase. In order to understand the continuum, we performed constant $\hbar\omega=1$ meV around (1,0,0) at several temperatures and along different $\vec{Q}$ directions. Shown in

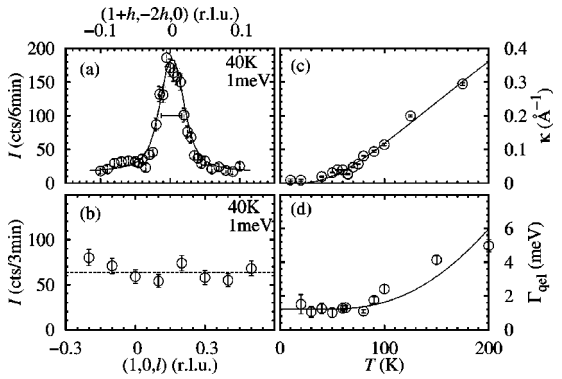

FIG. 5. Constant $\hbar\omega=1$ meV scan (a) along the $(1+h, -2h,0)$ direction and (b) along the $(1,0,l)$ direction at $T=40$ K. The horizontal bar in (a) represents the instrumental resolution. T dependence of (c) the intrinsic peak width, κ, obtained from the constant $\hbar\omega=1$ meV scans the along $(1+h,-2h,0)$ direction, and (d) the relaxation rate Γ_{qel} obtained from the constant $\vec{Q}=(1,0,0)$ scans shown in Fig. 3. Lines are explained in the text.

Figs. 5(a) and 5(b) are representative scans at $T=40$ K. A nearly resolution-limited peak is seen along the in-plane $(1+h,-2h,0)$ direction whereas the intensity is independent of l perpendicular to the plane. These indicate that the quasielastic component is purely 2D in nature, well localized at the 2D antiferromagnetic zone center. Figure 5(c) shows the temperature dependence of the intrinsic peak width along the $(1+h,-2h,0)$ direction. For $T>T_N$ the width decreases almost linearly, whereas it becomes nearly resolution limited below T_N, indicating a large in-plane correlation length at low temperatures. The energy width Γ_{qel} of the quasielastic peak is also shown in Fig. 5(d). Γ_{qel} decreases as T decreases down to T_N and saturates to a value of $\Gamma_{qel}\simeq 1.2(1)$ meV below T_N. It is surprising that the fast spin fluctuations with the characteristic time scale of $\tau_{qel}=\hbar/\Gamma_{qel}\sim 0.55(5)$ ps coexist with the long-lived spin waves in the 3D ordered Néel phase.

Because of the noncentrosymmetric crystal structure, $YMnO_3$ is known to show formation of crystallographic domains.[17] Thus, one might think it possible that the presently observed 2D fluctuations originate from certain crystallographic domains where 3D magnetic ordering is somehow suppressed even below T_N. However, the domains are magnetically equivalent, and thus spins in different domains should order equally at the same temperature; indeed, the entire sample is known to establish antiferromagnetic Néel order in $YMnO_3$ below T_N.[18] Therefore, the existence of the crystallographic domains is irrelevant for the coexisting two kinds of spin fluctuations; the 2D spin fluctuations intrinsically coexist with the conventional spin waves in the 3D ordered Néel phase.

What is the origin of the fast 2D fluctuations in the Néel phase? Recently, a similar quasielastic peak, called the *central peak*, has been found in numerical simulation studies on 2DXYTLAFMs.[19] Theoretically, such a central peak has been commonly seen in 2D *XY* spin systems, triangular or nontriangular, and is related to the vortex dynamics intrinsic to the KT phase.[20] We thus fitted our κ and Γ_{qel} to the phenomenological functions: $\kappa=\kappa_0\exp(-b/\sqrt{\tau})$ and $\Gamma=\Gamma_0+A\pi(\Lambda/\hbar)e^{-2b/\sqrt{\tau}}\{(\sqrt{2}-1)[\ln(k_BT_{KT}/\Lambda)/2+b/\sqrt{\tau}]\}^{1/2}$, where $\tau=(T-T_{KT})/T_{KT}$ and $\Lambda=JS^2a^2\kappa_0^2/4$. Here if $A=1$ and $\Gamma_0=0$, κ and Γ reduce to the analytical expressions for the 2D *XY* square lattice system.[21] The best fit [solid lines in Figs. 5(c) and 5(d)] was obtained with $T_{KT}=11(10)$ K, $b=10(4)$, $\kappa_0=4(1)$ Å^{-1}, $A=0.07(1)$, and $\Gamma_0=1.2(1)$ meV. The fit reproduces κ and Γ well for the entire temperature range, suggesting that the quasielastic peak is reminiscence of the vortex dynamics. Coexistence of the magnons and quasielastic peak suggests competition between the Néel phase favored by the weak interplane interactions and the KT phase intrinsic to the 2D *XY* spin system at low temperatures. It remains to be seen whether or not the prefactor A being smaller than 1 and the nonzero Γ_0 for the relaxation rate are intrinsic to the 2DXYLTAFMs or are due to the competition between the two phases.[22]

IV. SUMMARY

Spin excitations in the hexagonal antiferromagnet $YMnO_3$ have been studied using the inelastic neutron-scattering technique. We observed a quasielastic central peak at the 2D AFM zone center in the Néel phase, coexisting with the conventional 3D antiferromagnetic spin waves. The central peak bears characteristics of the KT phase intrinsic to the 2D *XY* spin systems. Understanding in detail how the Néel and KT phases compete and change the nature of the dynamic spin correlations would require further theoretical and experimental studies in the 2D *XY* spin systems.

ACKNOWLEDGMENTS

The authors thank K. Nho for providing us details of their theoretical calculations. Work at SPINS and DCS was partially supported by the NSF under Grant Nos. DMR-9986442 and DMR-0086210, respectively. The stay of T.J.S. at NIST was partially supported by the Atomic Energy Division, Ministry of Education, Culture, Sports, Science, and Technology, Japan.

*On leave from National Institute for Materials Science, Tsukuba 305-0047, Japan. Email address: tjsato@nist.gov

[1] A.P. Ramirez, in *Handbook on Magnetic Materials*, edited by K.J.H. Busch (Elsevier Science, Amsterdam, 2001), Vol. 13, p. 423.

[2] S.-H. Lee, C. Broholm, W. Ratcliff, G. Gasparovic, Q. Huang, T.H. Kim, and S.-W. Cheong, Nature (London) **418**, 856 (2002).

[3] *Magnetic Properties of Layered Transition Metal Compounds*, edited by L.J. de Jongh and R.D. Willet (Reidel, Dordrecht, 1987).

[4] H. Kawamura, J. Phys.: Condens. Matter **10**, 4707 (1998).

[5] J.M. Kosterlitz and D.J. Thouless, J. Phys. C **6**, 1181 (1973).

[6] See M.F. Collins and O.A. Petrenko, Can. J. Phys. **75**, 605 (1997) for an extensive review of experiments on TLAFMs. One may note that there are only a few model compounds for 2DT-

LAFMs; earlier studies are mostly on three-dimensional systems, such as the nonoxide ABX_3 magnets, which apparently lack the two dimensionality.

[7] T. Katsufuji, M. Masaki, A. Machida, M. Moritomo, K. Kato, E. Nishibori, M. Takata, M. Sakata, K. Ohoyama, K. Kitazawa, and H. Takagi, Phys. Rev. B **66**, 134434 (2002).

[8] A. Muñoz, J.A. Alonso, M.J. Martínez-Lope, M.T. Casáis, J.L. Martínez, and M.T. Fernández-Díaz, Phys. Rev. B **62**, 9498 (2000).

[9] T. Katsufuji, S. Mori, M. Masaki, Y. Moritomo, N. Yamamoto, and H. Takagi, Phys. Rev. B **64**, 104419 (2001).

[10] M. Bieringer and J.E. Greedan, J. Solid State Chem. **143**, 132 (1999).

[11] S.W. Lovesey, *Theory of Neutron Scattering from Condensed Matter* (Clarendon, Oxford, 1984), Vol. 2.

[12] S.-H. Lee, C. Broholm, T.H. Kim, W. Ratcliff II, and S.-W. Cheong, Phys. Rev. Lett. **84**, 3718 (2000).

[13] We rule out the phonon as the origin because intensity does not follow the Q^2 behavior.

[14] R. M. White, M. Sparks, and I. Ortenburger, Phys. Rev. **139**, A450 (1965).

[15] J. Takahashi, K. Hagita, K. Kohn, Y. Tanaba, and E. Hanamura, Phys. Rev. Lett. **89**, 076404 (2002).

[16] M.N. Iliev, V.G. Hadjiev, A.P. Litvinchuk, and R.L. Meng, Phys. Rev. Lett. **90**, 069701 (2003).

[17] M. Fiebig, D. Fröhlich, T. Lottermoser, and M. Matt, Phys. Rev. B **66**, 144102 (2002).

[18] M. Fiebig, D. Fröhlich, S. Leute, and R.V. Pisarev, J. Appl. Phys. **83**, 6560 (1998).

[19] K. Nho and D.P. Landau, Phys. Rev. B **66**, 174403 (2002).

[20] J.E.R. Costa and B. V. Costa, Phys. Rev. B **54**, 994 (1996).

[21] F.G. Mertens, A.R. Bishop, G.M. Wysin, and C. Kawabata, Phys. Rev. B **39**, 591 (1989).

[22] S. Sachdev, Science **288**, 475 (2000).